LAWRENCE
LIVERMORE
NATIONAL
LABORATORY

LLNL-CONF-724957

Effect of stereoisomeric structure and bond location on the ignition and reaction pathways of hexane isomers

C. Liu, C. L. Barraza-Botet, S. W. Wagnon, M. S. Wooldridge

February 22, 2017

10th US National Combustion Meeting
College Park, MD, United States
April 23, 2017 through April 26, 2017

Disclaimer

10th U. S. National Combustion Meeting
Organized by the Eastern States Section of the Combustion Institute
April 23-26, 2017
College Park, Maryland

Effect of stereoisomeric structure and bond location on the ignition and reaction pathways of hexenes

Changpeng Liu[1], Cesar L. Barraza-Botet[2], Scott W. Wagnon[3], Margaret S. Wooldridge[2,]*

[1]State Key Laboratory of Automotive Safety and Energy, Tsinghua University, Beijing 100084, China
[2]Department of Mechanical Engineering, University of Michigan, Ann Arbor, MI 48109, USA
[3]Lawrence Livermore National Laboratory, Livermore, CA 94550, USA
[*]Corresponding Author Email: mswool@umich.edu

Abstract: The current work presents new experimental autoignition and speciation data on the two cis-hexenes isomers (cis-2-hexene and cis-3-hexene). The new data together with previous data on the trans-hexene isomers describe the effect of the location of the carbon-carbon double bond and stereoisomeric structures on the reaction pathways of the linear isomers. Experiments were conducted with the University of Michigan rapid compression facility to determine ignition delay times from pressure histories. Stoichiometric (ϕ = 1.0) mixtures at dilution levels of buffer gas:O_2 = 7.5 (mole basis) were investigated at an average pressure of 11 atm and temperatures from 803 to 1052 K. The ignition delay time showed negligible sensitivity to the location of the carbon-carbon double bond and the stereoisomeric structure (cis-trans) for the conditions considered, consistent with expectations for alkenes at high temperatures (> 900 K). Model predictions using the Lawrence Livermore National Laboratory reaction mechanism (developed for gasoline surrogate combustion, which includes hexene reaction pathways) for ignition delay times and intermediate species were in generally good agreement with the experimental data. However, the mechanism for 3-hexene significantly over-predicted the formation of small aldehyde (C_2-C_4) species for both stereoisomers.

Keywords: hexene isomers, ignition, gas chromatography

1. Introduction

In addition to alcohols, biodiesel fuels are promising alternatives to petroleum derived fuels, particularly if they can be produced from feed stocks that do not compete with food crops. The esters in biodiesel fuels are long chain, typically C_{18} species,

LLNL-CONF-724957

and the majority (typically over 50%) are unsaturated compounds [1,2]. In addition, the unsaturated esters found in biodiesel fuels are often cis-isomers of the compounds [3]. Few studies have examined the combustion behavior of stereoisomeric (cis-trans) olefins [4,5], and, to our knowledge, no studies have investigated the effects of stereoisomerism coupled with an ester moiety. An example of the cis-trans alkene isomer structures is provided in Figure 1 for the linear hexene stereoisomers.

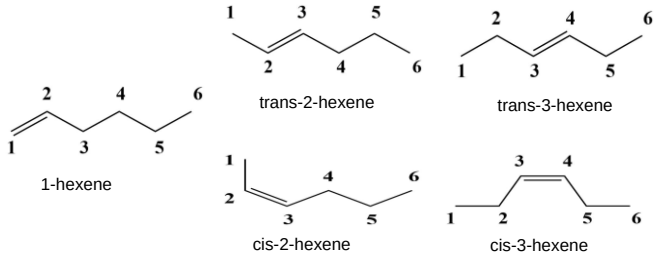

Figure 1. Structures of the linear hexene isomers

In a recent study, Hellier et al. [6] investigated octene isomers (including cis and trans-3-octene) in a single cylinder direct injection diesel engine. Hellier et al. [6] concluded trans-3-octene ignited slower than cis-3-octene at the conditions of their study because the trans form of the olefins must isomerize to a cis configuration prior to proceeding through low temperature reaction pathways, in agreement with prior studies by Salooja [4] and Bounaceour et al. [7]. Fridyland et al. [5] found the results for the two cis-trans isomers were indistinguishable for the conditions of their study. It is unclear based on the available literature whether proposed biodiesel surrogates should consist of cis or trans (or both) compounds to appropriately capture the combustion kinetics of real biodiesel fuels, and studies of both isomeric forms provide insight into appropriately representing biodiesel chemistry.

Recently, the combustion behavior and chemical kinetics of the three trans isomers of hexene (C_6H_{12}) have been studied experimentally and computationally [7-9], including ignition studies using the University of Michigan rapid compression facility (UM RCF) [10, 11]. These studies provide a foundation for comparison and further motivate the current study of the low-temperature behavior of the cis-hexene isomers in order to understand the potential impact of stereoisomers on fossil fuel and biofuel combustion kinetics.

2. Experimental and Computational Approach

The experimental procedure for the cis-hexene study was the same as used for the trans-hexene study described in Wagnon et al. [11]. Ignition imaging and gas-sampling experiments were conducted. Detailed descriptions of the gas chromatography equipment and procedures are provided in the Supporting Information.

Computational simulations were carried out using the CHEMKIN suite (version 10131, x64) [12] of programs and assuming a closed zero-dimensional homogeneous batch reactor at adiabatic, constant volume conditions. The appropriateness of these modeling assumptions has been considered previously for UM RCF experiments [13, 14] and by others [15] and the appropriateness was confirmed in this study. Autoignition simulations of the hexene isomers were conducted using the Lawrence Livermore National Laboratory (LLNL) gasoline surrogate chemical kinetic

LLNL-CONF-724957

mechanism developed by Mehl et al. [9] which includes hexene reaction pathways. No modifications to any of the reaction rates were made in this study.

3. Results and Discussion

Ignition delay times. A summary of the measured ignition delay times for the five hexene isomers is presented in Figure 2. Experimental conditions for each fuel were fixed at a stoichiometric fuel-to-O_2 equivalence ratio (ϕ = 1.0) and dilution of buffer gas:O_2 = 7.5 (molar basis). The current study focused on a limited range of pressure (from P = 10.1 to 11.5 atm with an average value of P = 11 atm) and temperatures from T = 809 to 1052 K. The experimental data of Figure 2 have been scaled to the molar dilution ratio of 7.5 and P = 11 atm, using $\tau_{ign} \propto P^{-1}$ and $\tau_{ign} \propto$ (the mole fraction ratio of the inert gases to O_2 in the reactant mixture). The scaling rules are based on trends observed in previous ignition studies [13,15] and are considered accurate for data outside the negative temperature coefficient region of the fuels. The recommended uncertainty of ±16% in the ignition delay times is shown as the error bars in Figure 2 and is attributed primarily to the accuracy of the pressure transducer (±<0.4% full scale) in the test section.

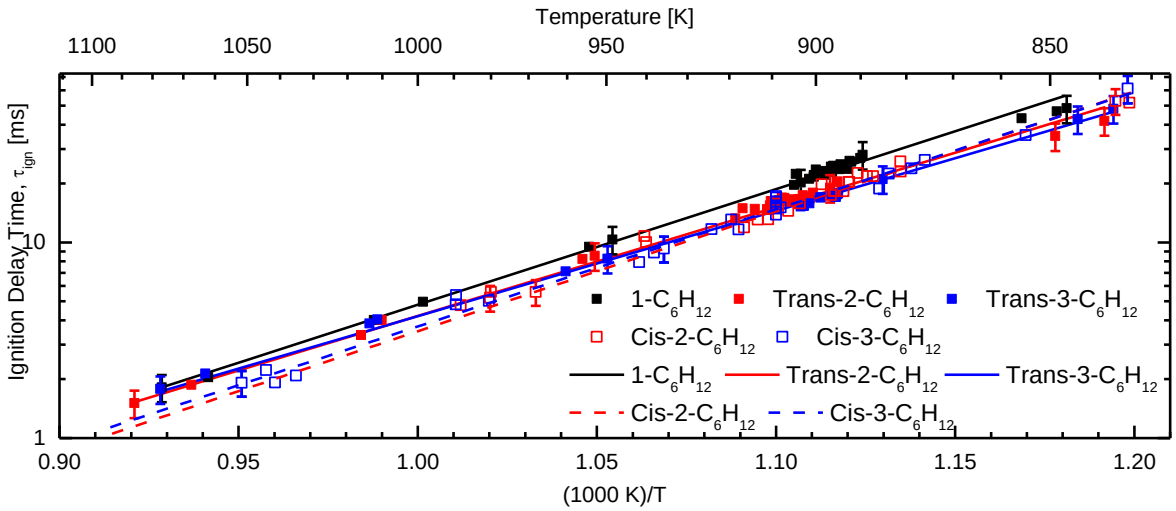

Figure 2. Comparison of the ignition delay time measurements (symbols) of 1-hexene, trans-2-hexene, trans-3-hexene, cis-2-hexene, and cis-3-hexene. Linear regressions for each isomer data set are presented as lines.

The results in Figure 2 show the five hexene isomers exhibited negligible difference in ignition delay times indicating the reactivity is nearly identical in the current temperature range. Arrhenius behavior was observed for 2-hexene and 3-hexene throughout the range of temperatures studied and for temperatures above 875 K for 1-hexene. When the temperature was lower than 875 K, 1-hexene showed a slight increase in reactivity and decrease in activation energy, which is consistent with theory and previous studies, indicating the possible onset of non-Arrhenius behavior at these conditions. The lines showed in Figure 1 are best-fit regression correlations of the form $\tau_{ign} = Aexp(E_a/RT)$.

Intermediate Species. Results from the fast sampling for the five hexene fuels are shown in Figures 3-5 for the hexene isomers, propanal (C_2H_5CHO), and 1,3-

LLNL-CONF-724957

butadiene, respectively. The average state conditions for the sampling experiments were P = 11.1 atm, T = 911 K for cis-2-hexene and P = 10.8 atm, T = 903 K for cis-3-hexene. Additional stable intermediate species measurements are provided in the Supporting Information for carbon monoxide, methane, methanol, ethene, ethane, ethyne, ethanol, propene, 1-pentene and methacrolein. The experimental data for the hexene fuels show the rates of consumption were similar for all five isomers, with a rapid increase in the rate of consumption late in the ignition delay time period (t/τ_{ign}>0.9). In general, the experimental data and model predictions agreed quite well and were within the ±20% uncertainties of the hexene measurements throughout the time histories.

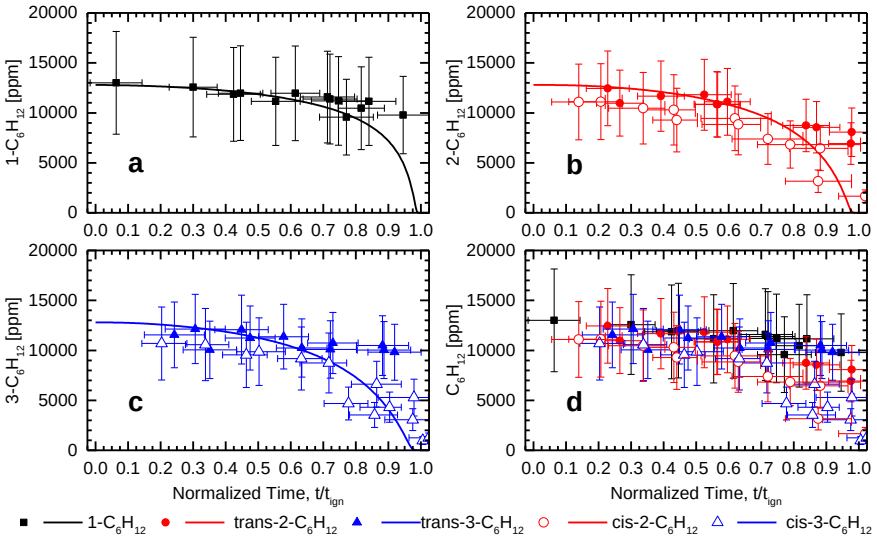

Figure 3. Measured (symbols) and predicted (lines) time histories of a) 1-hexene b) 2-hexene, and c) 3-hexene and 4) all data. Open symbols indicate measurements from the cis-hexene isomer experiments.

The cis- and trans- experimental data for propanal (C_2H_5CHO) were indistinguishable, and the experimental data showed the propanal production decreased for the longer alkyl chain isomers (1-hexene and 2-hexene) relative to the 3-hexenes. For 1-hexene and 2-hexene, the model predictions and experimental data for propanal agreed well, within a factor of ~2. However, for 3-hexene, the simulations over-predicted the experimental measurements for propanal during ignition delay by more than a factor of 10. This over-prediction may be related to the rate of the H-atom abstraction reaction from the initial hexene, where the rate may be too high for the 3-hexene isomer.

Figure 5 shows the measurements and model predictions for 1,3-butadiene (C_4H_6-1,3). Again, there were no obvious differences between the trans-hexene and cis-hexene data. The model predicted the 1,3-butadiene time histories for 1-hexene and 2-hexene very well. However, the model over-predicted the results for the 3-hexene isomers by more than a factor of ~8. The experimental data indicate the longer alkyl chain significantly promoted 1,3-butadiene production (a factor of ~10 increase in production for 1-hexene and 2-hexene compared with 3-hexene at t/τ_{ign}=0.9).

LLNL-CONF-724957

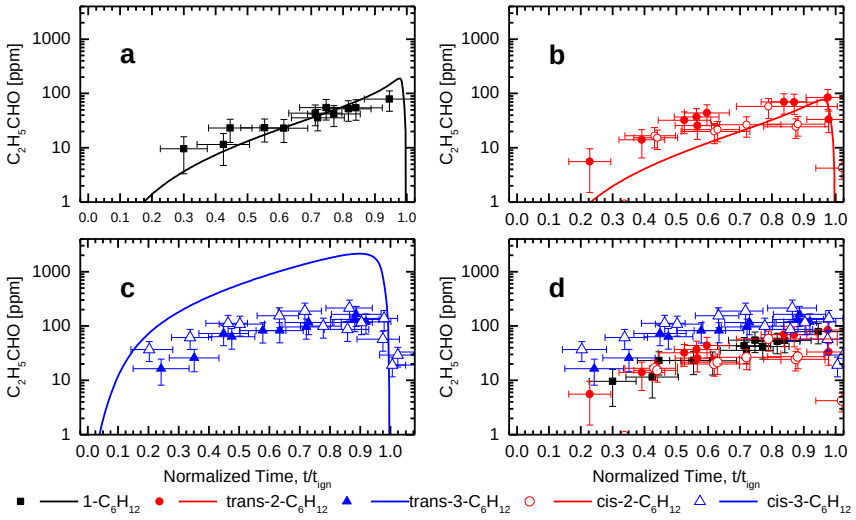

Figure 4. Measured (symbols) and predicted (lines) time histories of propanal from ignition of a) 1-hexene b) 2-hexene, and c) 3-hexene and 4) all data. Open symbols indicate measurements from the cis-hexene isomer experiments.

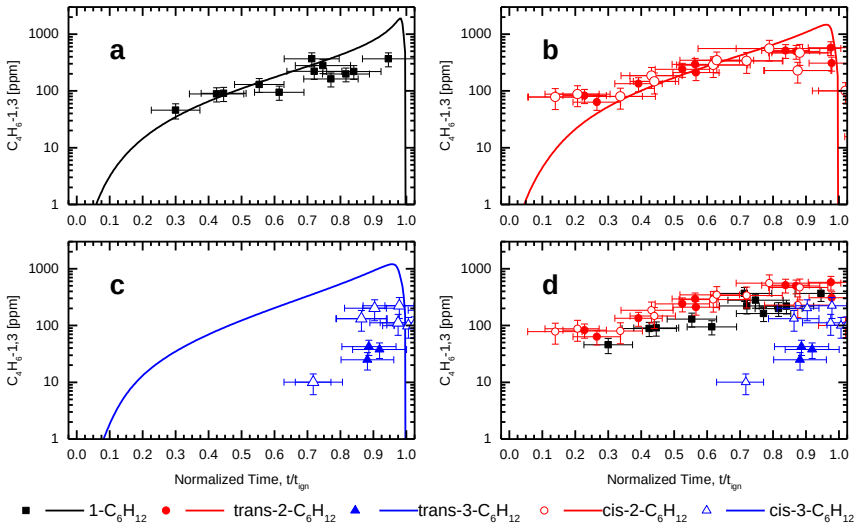

Figure 5. Measured (symbols) and predicted (lines) time histories of 1,3-butadiene from ignition of a) 1-hexene b) 2-hexene, and c) 3-hexene and 4) all data. Open symbols indicate measurements from the cis-hexene isomer experiments.

4. Conclusions

The new ignition delay time data for cis-2-hexene and cis-3-hexene presented in this work together with other ignition delay data for trans-hexenes [11] show negligible sensitivity to the location of the carbon-carbon double bond and stereoisomeric structure (cis-trans) for the state and mixture conditions considered. However, the measurements of some stable intermediates showed significant differences in the isomer reaction pathways. The stereoisomeric (cis-trans) structure had little effect on reaction pathways, while the carbon-carbon double bond did affect the reaction processes. A longer alkyl chain significantly promoted 1,3-butadiene production (a factor of ~10 increase in production for 1-hexene and 2-hexene compared with 3-hexene), and decreased the propanal production by a factor of ~3. Generally, model predictions for ignition delay times and intermediate species were in good agreement

with the experimental data. However, the mechanism for 3-hexene significantly over-predicted the formation of small aldehyde (C_2-C_4) species for both stereo isomers. Current work includes analysis of the results to identify the specific reaction pathways and rates affected by the alkyl chain length.

5. Acknowledgements

The authors acknowledge the support of the US. Department of Energy Office (DOE) of Basic Energy Sciences via Contract DE-SC0002645. Portions of this work were performed under the auspices of the U.S. DOE by LLNL under Contract DE-AC52-07NA27344 through the Special Employee Strategic Mission Support program.

6. References

[1] O. Herbinet, W.J. Pitz, C.K. Westbrook, Detailed chemical kinetic oxidation mechanism for a biodiesel surrogate, Combustion and Flame 154 (2008) 507-28.

[2] S.K. Hoekman, A. Broch, C. Robbins, et al., Review of biodiesel composition, properties, and specifications, Renewable and Sustainable Energy Reviews 16 (2012) 143-69.

[3] L. Coniglio, H. Bennadji, P.A. Glaude, et al., Combustion chemical kinetics of biodiesel and related compounds (methyl and ethyl esters): Experiments and modeling – Advances and future refinements, Progress in Energy and Combustion Science 39 (2013) 340-82.

[4] K.C. Salooja, Combustion studies of olefins and of their influence on hydrocarbon combustion processes, Combustion and Flame 12 (1968) 401-10.

[5] A. Fridlyand, S.S. Goldsborough, K. Brezinsky, et al., Influence of the double bond position on the oxidation of decene isomers at high pressures and temperatures, Proceedings of the Combustion Institute 35 (2015) 333-40.

[6] P. Hellier, N. Ladommatos, R. Allan, et al., The importance of double bond position and cis–trans isomerisation in diesel combustion and emissions, Fuel 105 (2013) 477-89.

[7] R. Bounaceur, V. Warth, B. Sirjean, et al., Influence of the position of the double bond on the autoignition of linear alkenes at low temperature, Proceedings of the Combustion Institute 32 (2009) 387-94.

[8] G. Vanhove, M. Ribaucour, R. Minetti, On the influence of the position of the double bond on the low-temperature chemistry of hexenes, Proceedings of the Combustion Institute 30 (2005) 1065-72.

[9] M. Mehl, W.J. Pitz, C.K. Westbrook, et al., Kinetic modeling of gasoline surrogate components and mixtures under engine conditions, Proceedings of the Combustion Institute 33 (2011) 193-200.

[10] S.W. Wagnon, chemical kinetics for advanced combustion strategies, PhD Dissertation University of Michigan, Ann Arbor, MI (2014).

[11] S.W. Wagnon, C.L. Barraza-Botet, M.S. Wooldridge, Effects of bond location on the ignition and reaction pathways of trans-hexene isomers, J Phys Chem A 119 (2015) 7695-703.

[12] CHEMKIN release 10131, Reaction Design., San Diego (2013).

[13] D.M.A. Karwat, S.W. Wagnon, M.S. Wooldridge, et al., Low-temperature speciation and chemical kinetic studies of n-heptane, Combustion and Flame 160 (2013) 2693-706.

[14] A.B. Mansfield, M.S. Wooldridge, High-pressure low-temperature ignition behavior of syngas mixtures, Combustion and Flame 161 (2014) 2242-51.

[15] J. Würmel, E.J. Silke, H.J. Curran, et al., The effect of diluent gases on ignition delay times in the shock tube and in the rapid compression machine, Combustion and Flame 151 (2007) 289-302.

Supporting Information

Effect of stereoisomeric structure and bond location on the ignition and reaction pathways of hexane isomers

Changpeng Liu[1], Cesar L. Barraza-Botet[2], Scott W. Wagnon[3], Margaret S. Wooldridge[2, *]

[1]State Key Laboratory of Automotive Safety and Energy, Tsinghua University, Beijing 100084, China

[2]Department of Machanical Engineering, University of Michigan, Ann Arbor, Michigan 48109, United States

[3]Lawrence Livermore National Laboratory, Livermore, California 94550, United States

Table S1. Gas chromatography specifications and temperature methods for ethanol speciation experiments

ID No.	Column	Length	ID	Film	Carrier Gas	T_{column}	Detector	$T_{detector}$
GC-1 /FID	CP-Porabond Q	25 m	0.53 mm	10 um	Helium 31 cm/s	40 ℃ (2 min) 6 ℃ /min 160℃(3 min)	FID	300℃
GC-2 /FID	CP-Al_2O/Na_2SO_4	25 m	0.53 mm	10 um	Helium 32 cm/s	40 ℃ (2 min) 6 ℃ /min 160℃(3 min)	FID	300℃
GC-3 /FID	DB-WAX	30 m	0.25 mm	0.25 um	Helium 70 cm/s	40 ℃ (2 min) 6 ℃ /min 160℃(3 min)	FID	300℃
GC-3 /TCD	ShinCarbon ST	2 m	1 mm	N/A	Helium 19 mL/min	40 ℃ (2 min) 6 ℃ /min 160℃(3 min)	TCD	100℃

Table S2. Summary of experimental conditions and results for cis-2-hexene autoignition. All mixture data are provided on a mole fraction basis.

ø	Inert :O_2	Test Gas Composition					Peff	Teff	τ_{ign}
		χ (cis-2-C_6H_{12}) [%]	χ (O_2) [%]	χ (N_2) [%]	χ (Ar) [%]	χ (CO_2) [%]	[atm]	[K]	[ms]
0.99	7.49	1.28	11.62	86.94	0	0.15	10.5	940	10.0
0.99	7.49	1.28	11.62	86.94	0	0.15	10.5	941	10.8
0.99	7.49	1.28	11.62	78.09	0	9.0	10.4	887	21.8
0.99	7.49	1.28	11.65	78.09	0.01	8.98	10.6	891	22.6
0.99	7.49	1.28	11.63	74.88	12.21	0	10.1	980	5.6
0.99	7.49	1.28	11.64	74.88	12.21	0	10.3	980	5.2
0.99	7.49	1.28	11.62	67.5	0	19.59	10.4	834	51.8
0.99	7.49	1.28	11.62	67.5	0	19.59	9.2	809	95.1

LLNL-CONF-724957

0.99	7.49	1.28	11.62	82.48	0	4.61	11.2	896	18.3
0.99	7.49	1.28	11.62	82.48	0	4.62	11.1	894	18.2
0.99	7.49	1.28	11.62	82.48	0	4.62	11.3	897	17.5
0.99	7.49	1.28	11.62	82.47	0	4.61	10.8	889	21.8
0.99	7.49	1.28	11.62	82.47	0	4.62	10.5	881	23.0
0.99	7.49	1.28	11.66	78.13	0	8.94	10.6	899	19.8
0.99	7.49	1.28	11.66	74.58	12.26	0	10.5	988	4.8
0.99	7.49	1.28	11.63	81.70	5.38	0	11.6	968	5.6
0.99	7.49	1.28	11.64	83.54	0	3.53	10.54	893	20.4
0.99	7.49	1.28	11.63	85.38	0	1.69	10.8	904	15.8
0.99	7.49	1.28	11.63	85.38	0	1.69	10.4	896	18.4
0.99	7.49	1.28	11.63	86.70	0	0.38	11.0	906	14.5
0.99	7.49	1.28	11.63	86.70	0	0.38	10.4	893	20.4
0.99	7.49	1.28	11.63	86.74	0.33	0	11.3	911	13.1
0.99	7.49	1.28	11.63	86.74	0.33	0	11.5	917	11.9
0.99	7.49	1.28	11.64	86.74	0.33	0	10.9	913	13.1
0.99	7.49	1.28	11.64	86.74	0.33	0	10.9	913	13.1

Table S3. Summary of experimental conditions and results for cis-2-hexene autoignition. All mixture data are provided on a mole fraction basis.

ø	Inert :O_2	Test Gas Composition					Peff	Teff	τ_{ign}
		χ (cis-3-C_6H_{12}) [%]	χ (O_2) [%]	χ (N_2) [%]	χ (Ar) [%]	χ (CO_2) [%]	[atm]	[K]	[ms]
0.99	7.49	1.28	11.62	64.08	23.02	0	10.9	981	5.0
0.99	7.49	1.28	11.62	64.09	23.01	0	13.4	1035	2.0
0.99	7.49	1.28	11.61	64.08	23.05	0	13.6	1042	1.9
0.99	7.49	1.28	11.63	64.09	23.00	0	13.3	1044	2.2
0.99	7.49	1.28	11.66	74.85	12.21	0	10.8	989	5.4
0.99	7.49	1.28	11.61	86.96	0	0.14	10.4	936	9.4
0.99	7.49	1.28	11.61	86.96	0	0.15	9.8	920	13.3
0.99	7.49	1.28	11.62	86.95	0	0.15	10.4	924	11.7
0.99	7.49	1.28	11.62	78.10	0	8.99	10.2	876	26.6
0.99	7.49	1.28	11.62	78.10	0	8.99	10.9	884	22.5
0.99	7.49	1.28	11.64	68.77	0.01	18.30	10	821	76.3
0.99	7.49	1.28	11.63	68.76	0	18.32	10.8	835	61.1
0.99	7.49	1.28	11.65	82.46	0.01	4.61	11.9	908	14.8
0.99	7.49	1.28	11.65	85.58	1.47	0	11.1	938	8.8
0.99	7.49	1.28	11.64	76.69	0	10.37	10.1	855	35.8
0.99	7.49	1.28	11.65	61.69	25.36	0	11.7	1052	1.9
0.99	7.49	1.28	11.64	70.43	16.63	0	10.8	990	4.8
0.99	7.49	1.28	11.64	79.64	0	7.31	10.4	879	24
0.99	7.49	1.28	11.64	81.87	0	5.19	10.8	905	15.1
0.99	7.49	1.28	11.64	81.87	0	5.19	10.8	902	17.0
0.99	7.49	1.28	11.64	81.87	0	5.19	10.8	905	16.2

0.99	7.49	1.28	11.64	81.87	0	5.19	11.0	907	14.9
0.99	7.49	1.28	11.64	81.87	0	5.19	10.8	902	17.2
0.99	7.49	1.28	11.64	81.87	0	5.19	10.8	903	16.1
0.99	7.49	1.28	11.64	81.87	0	5.19	11.0	906	13.9
0.99	7.49	1.28	11.64	81.87	0	5.19	10.8	904	15.1
0.99	7.49	1.28	11.64	81.87	0	5.19	10.7	902	15.5

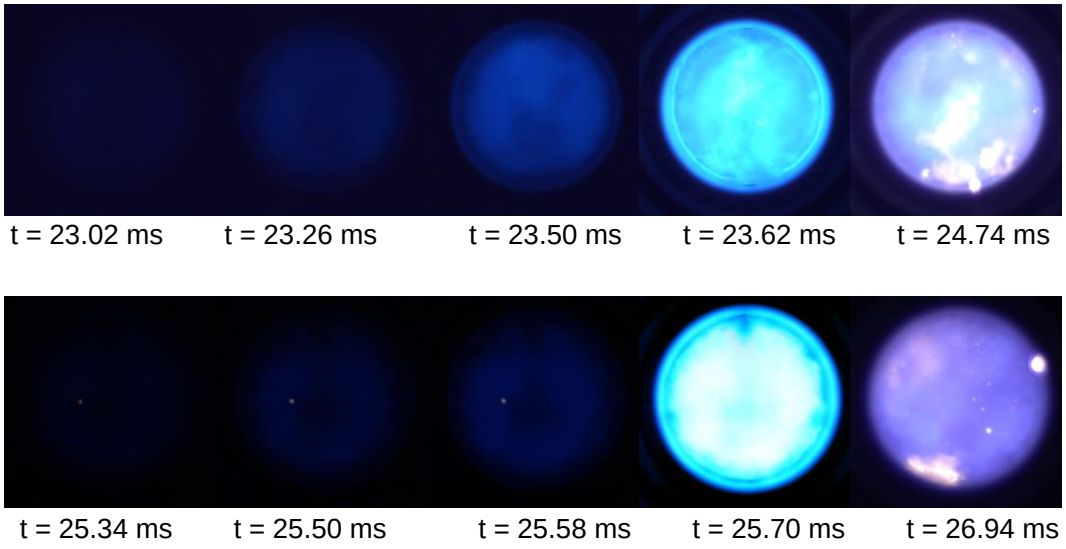

Figure S1. Still images from high speed imaging of the cis-2-hexene (top row) and cis-3-hexene (bottom row) UM RCF experiments at T_{eff} = ~900 K, P_{eff} = ~11 bar.

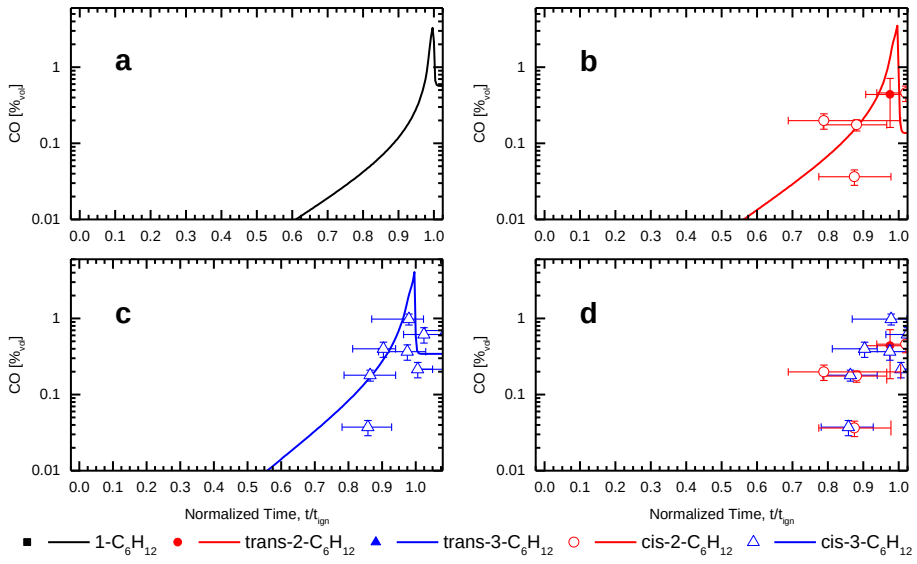

Figure S2. Measured (symbols) and predicted (lines) carbon monoxide (CO) time histories during autoignition of the five hexene isomers. Results are presented for mixtures of a) 1-hexene, b) trans-2-hexene and cis-2-hexene, c) trans-3-hexene and cis-3-hexene, and d) all five hexene isomers. Simulations for each isomer were calculated by Meth et al. mechanism at the average compositions and conditions of the experiments.

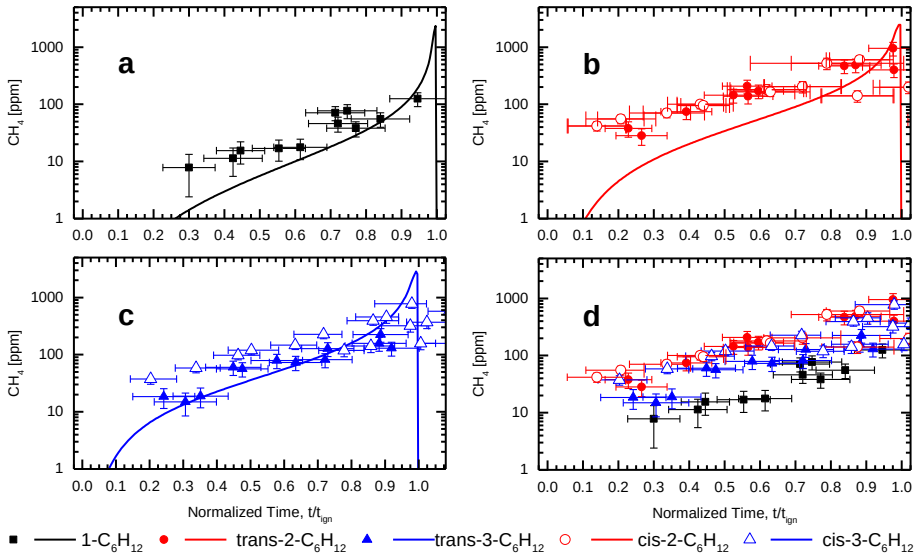

Figure S3. Measured (symbols) and predicted (lines) methane (CH_4) time histories during autoignition of the five hexene isomers. Results are presented for mixtures of a) 1-hexene, b) trans-2-hexene and cis-2-hexene, c) trans-3-hexene and cis-3-hexene, and d) all five hexene isomers. Simulations for each isomer were calculated by Meth et al. mechanism at the average compositions and conditions of the experiments.

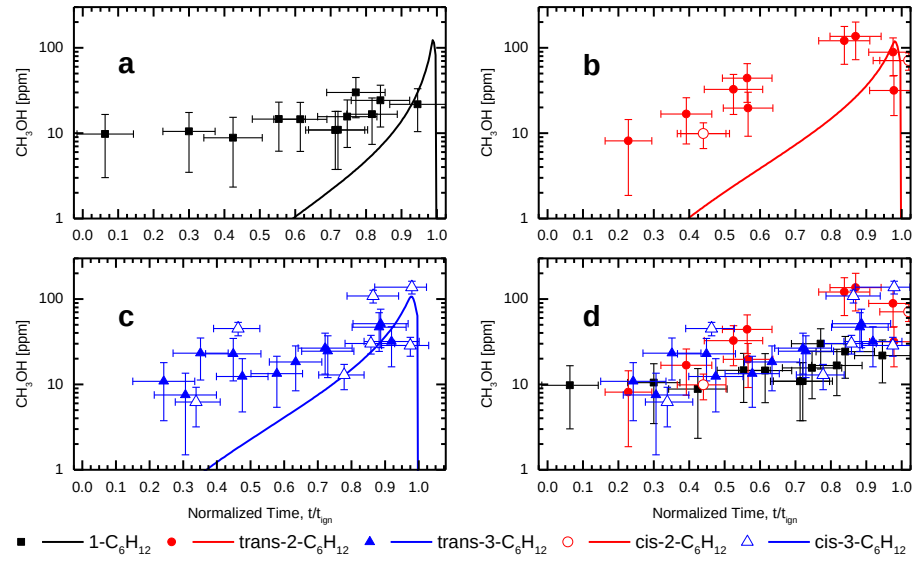

Figure S4. Measured (symbols) and predicted (lines) methanol (CH_3OH) time histories during autoignition of the five hexene isomers. Results are presented for mixtures of a) 1-hexene, b) trans-2-hexene and cis-2-hexene, c) trans-3-hexene and cis-3-hexene, and d) all five hexene isomers. Simulations for each isomer were calculated by Meth et al. mechanism at the average compositions and conditions of the experiments.

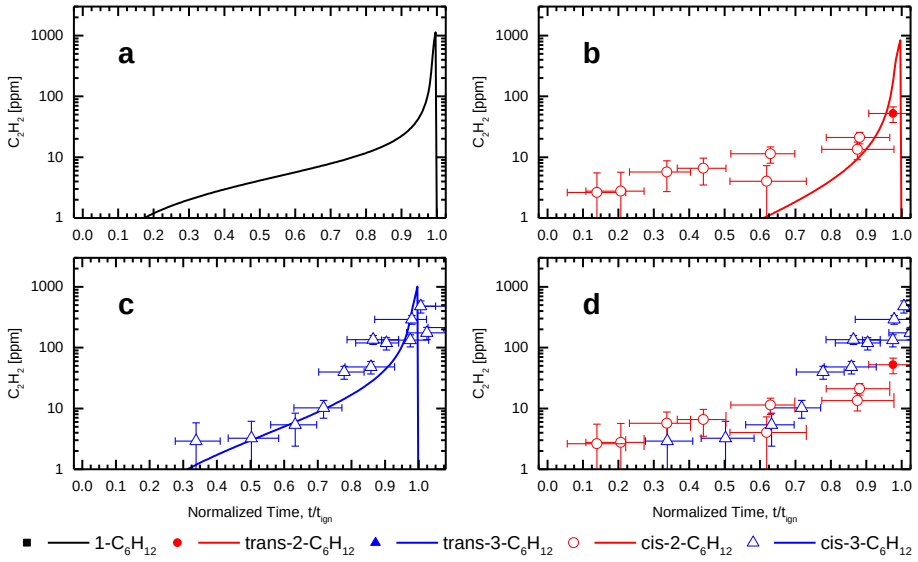

Figure S5. Measured (symbols) and predicted (lines) ethyne (C_2H_2) time histories during autoignition of the five hexene isomers. Results are presented for mixtures of a) 1-hexene, b) trans-2-hexene and cis-2-hexene, c) trans-3-hexene and cis-3-hexene, and d) all five hexene isomers. Simulations for each isomer were calculated by Meth et al. mechanism at the average compositions and conditions of the experiments.

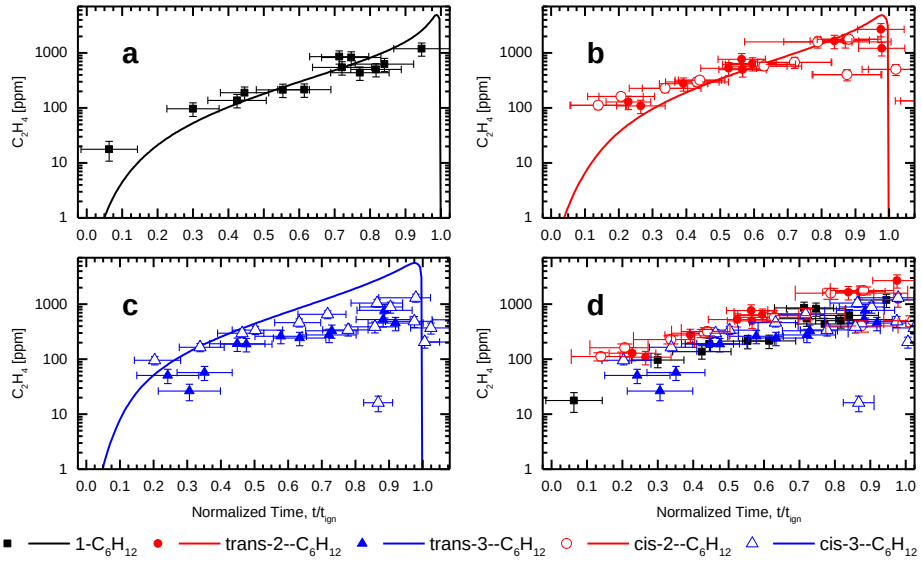

Figure S6. Measured (symbols) and predicted (lines) ethene (C_2H_4) time histories during autoignition of the five hexene isomers. Results are presented for mixtures of a) 1-hexene, b) trans-2-hexene and cis-2-hexene, c) trans-3-hexene and cis-3-hexene, and d) all five hexene isomers. Simulations for each isomer were calculated by Meth et al. mechanism at the average compositions and conditions of the experiments.

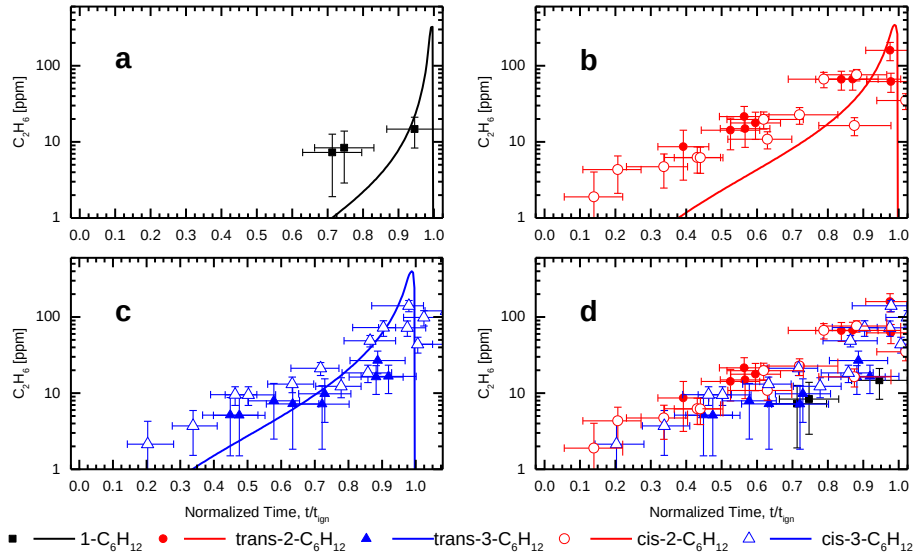

Figure S7. Measured (symbols) and predicted (lines) ethane (C_2H_6) time histories during autoignition of the five hexene isomers. Results are presented for mixtures of a) 1-hexene, b) trans-2-hexene and cis-2-hexene, c) trans-3-hexene and cis-3-hexene, and d) all five hexene isomers. Simulations for each isomer were calculated by Meth et al. mechanism at the average compositions and conditions of the experiments.

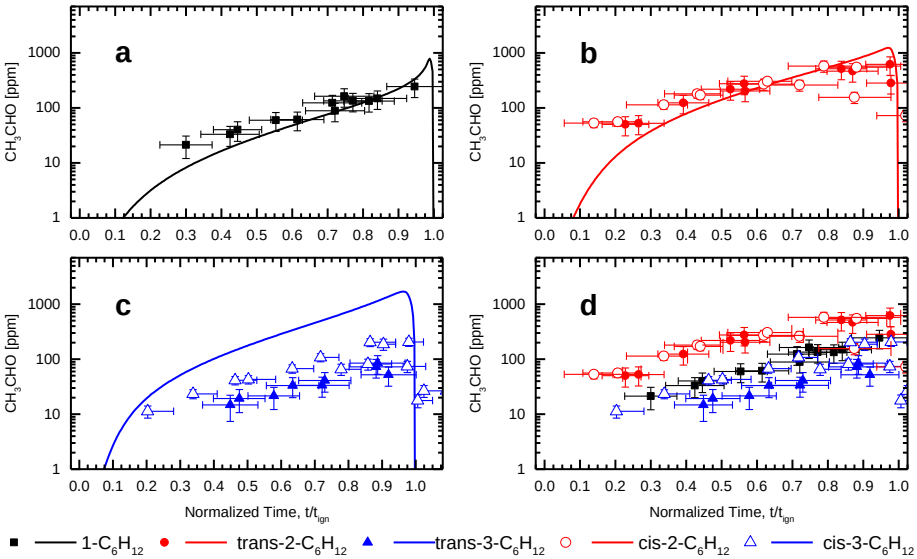

Figure S8. Measured (symbols) and predicted (lines) ethanal (CH_3CHO) time histories during autoignition of the five hexene isomers. Results are presented for mixtures of a) 1-hexene, b) trans-2-hexene and cis-2-hexene, c) trans-3-hexene and cis-3-hexene, and d) all five hexene isomers. Simulations for each isomer were calculated by Meth et al. mechanism at the average compositions and conditions of the experiments.

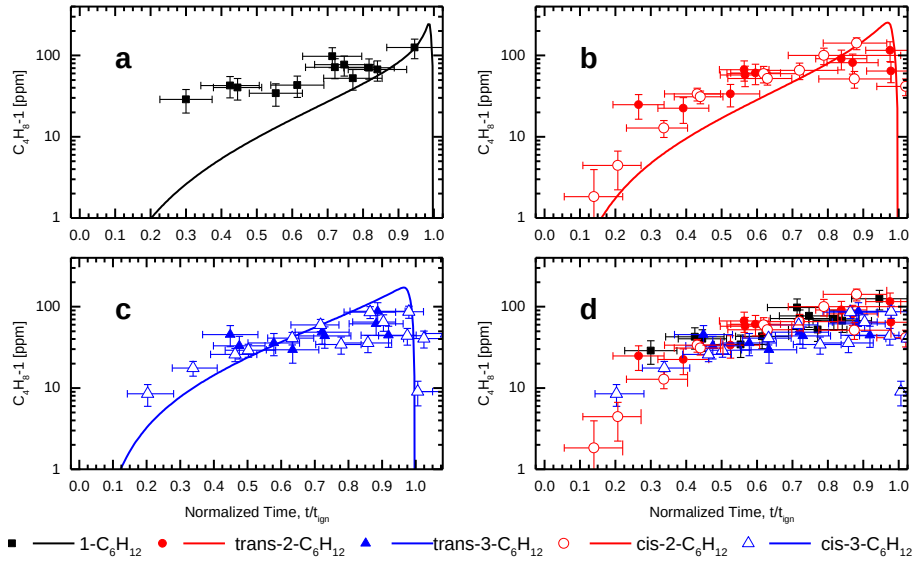

Figure S9. Measured (symbols) and predicted (lines) 1-butene (C_4H_8-1) time histories during autoignition of the five hexene isomers. Results are presented for mixtures of a) 1-hexene, b) trans-2-hexene and cis-2-hexene, c) trans-3-hexene and cis-3-hexene, and d) all five hexene isomers. Simulations for each isomer were calculated by Meth et al. mechanism at the average compositions and conditions of the experiments.

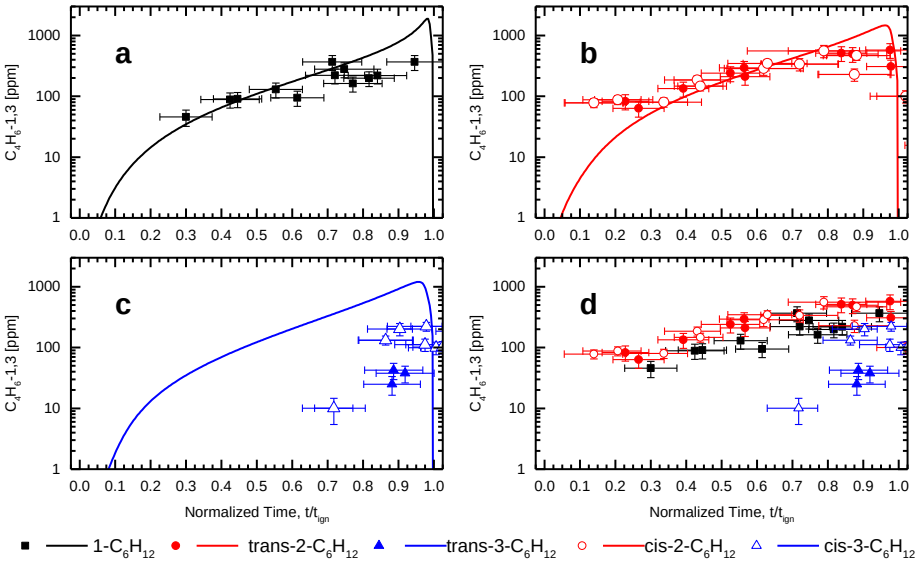

Figure S10. Measured (symbols) and predicted (lines) 1,3-butadiene (C_4H_6-1,3) time histories during autoignition of the five hexene isomers. Results are presented for mixtures of a) 1-hexene, b) trans-2-hexene and cis-2-hexene, c) trans-3-hexene and cis-3-hexene, and d) all five hexene isomers. Simulations for each isomer were calculated by Meth et al. mechanism at the average compositions and conditions of the experiments.

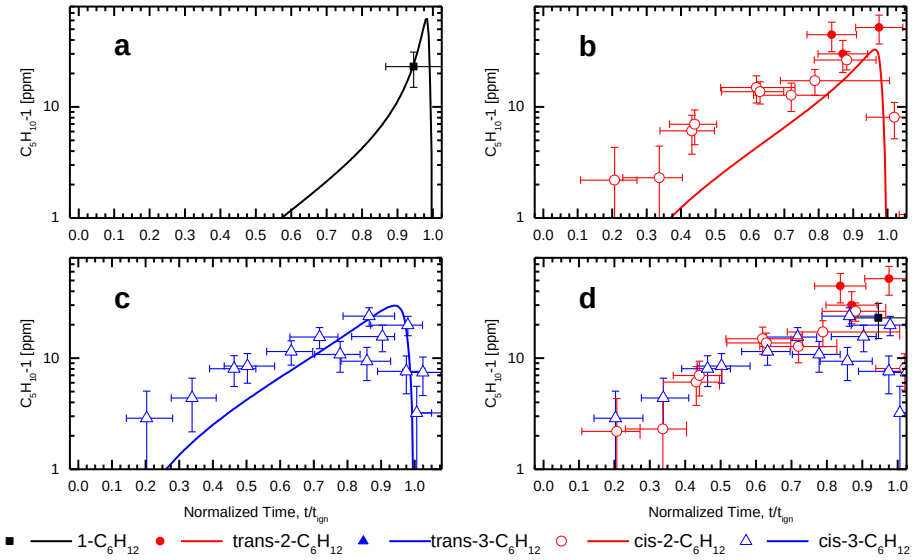

Figure S11. Measured (symbols) and predicted (lines) 1-pentene (C_5H_{10}-1) time histories during autoignition of the five hexene isomers. Results are presented for mixtures of a) 1-hexene, b) trans-2-hexene and cis-2-hexene, c) trans-3-hexene and cis-3-hexene, and d) all five hexene isomers. Simulations for each isomer were calculated by Meth et al. mechanism at the average compositions and conditions of the experiments.

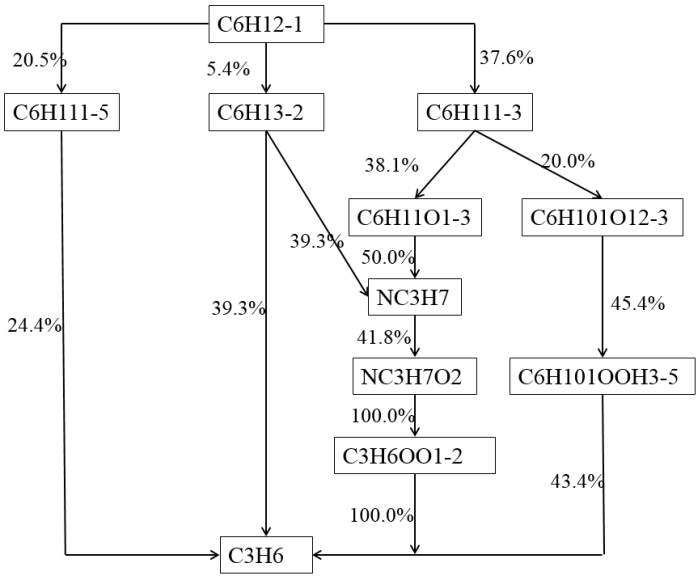

Figure S12. Reaction pathways based on the rate of production analysis for propene (C_3H_6) during the ignition of 1-hexene at a normalized time of $t/\tau_{ign} = 0.90$. Simulations were calculated with the Mehl et al. mechanism at average compositions and conditions of the experiments. Boxes indicate stable compounds in the reaction pathways.

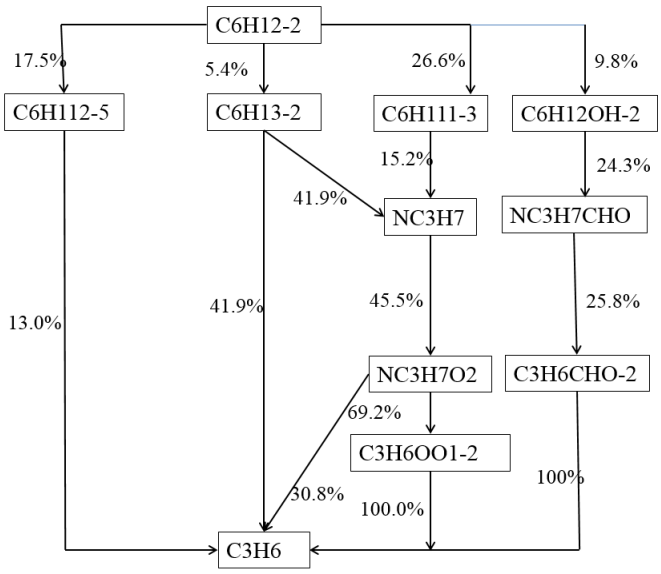

Figure S13. Reaction pathways based on the rate of production analysis for propene (C_3H_6) during the ignition of 2-hexene at a normalized time of $t/\tau_{ign} = 0.90$. Simulations were calculated with the Mehl et al. mechanism at average compositions and conditions of the experiments. Boxes indicate stable compounds in the reaction pathways.

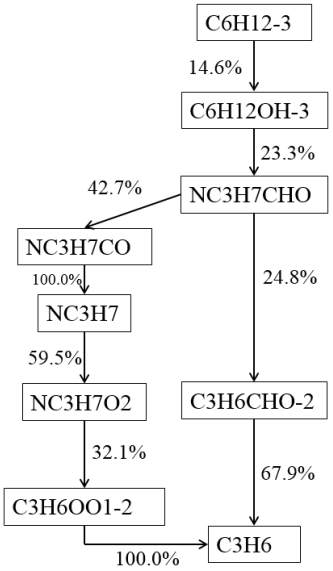

Figure S14. Reaction pathways based on the rate of production analysis for propene (C3H6) during the ignition of 3-hexene at a normalized time of $t/\tau_{ign} = 0.90$. Simulations were calculated with the Mehl et al. mechanism at average compositions and conditions of the experiments. Boxes indicate stable compounds in the reaction pathways.

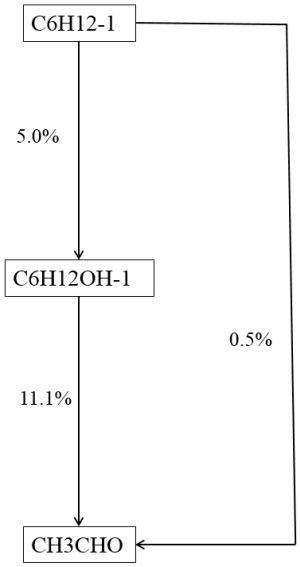

Figure S15. Reaction pathways based on the rate of production analysis for propene (CH_3CHO) during the ignition of 1-hexene at a normalized time of $t/\tau_{ign} = 0.90$. Simulations were calculated with the Mehl et al. mechanism at average compositions and conditions of the experiments. Boxes indicate stable compounds in the reaction pathways.

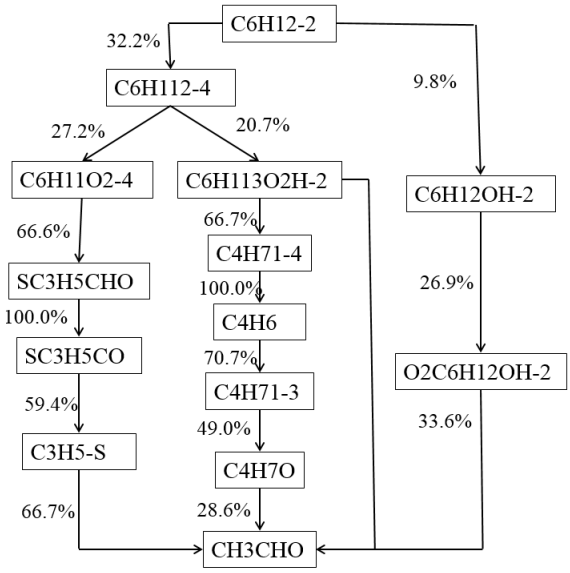

Figure S16. Reaction pathways based on the rate of production analysis for propene (CH_3CHO) during the ignition of 2-hexene at a normalized time of $t/\tau_{ign} = 0.90$. Simulations were calculated with the Mehl et al. mechanism at average compositions and conditions of the experiments. Boxes indicate stable compounds in the reaction pathways.

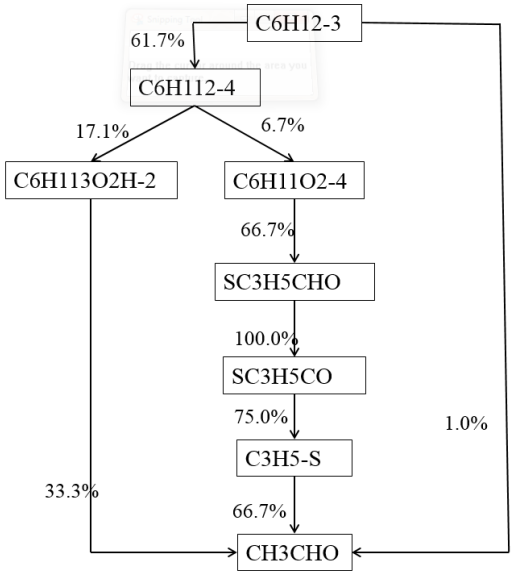

Figure S17. Reaction pathways based on the rate of production analysis for propene (CH_3CHO) during the ignition of 3-hexene at a normalized time of $t/\tau_{ign} = 0.90$. Simulations were calculated with the Mehl et al. mechanism at average compositions and conditions of the experiments. Boxes indicate stable compounds in the reaction pathways.

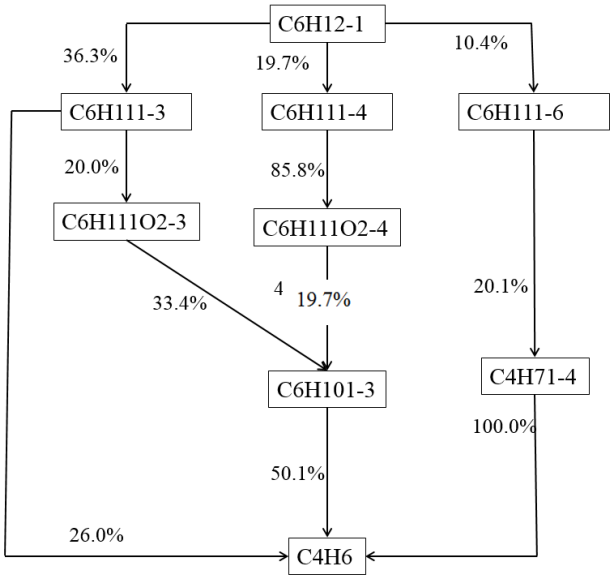

Figure S18. Reaction pathways based on the rate of production analysis for 1,3-butadiene (C_4H_6-1,3) during the ignition of 1-hexene at a normalized time of $t/\tau_{ign} = 0.90$. Simulations were calculated with the Mehl et al. mechanism at average compositions and conditions of the experiments. Boxes indicate stable compounds in the reaction pathways.

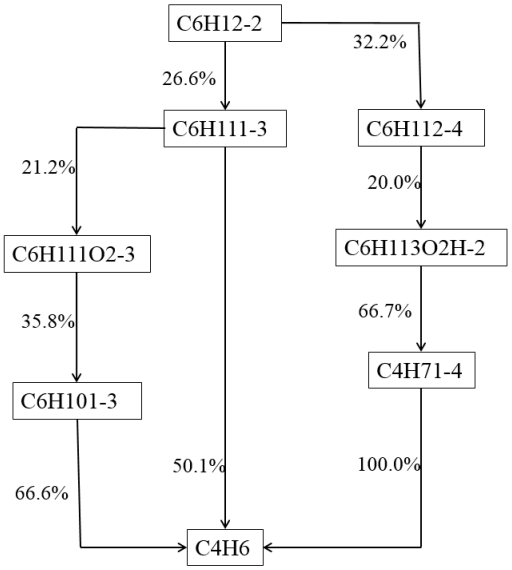

Figure S19. Reaction pathways based on the rate of production analysis for 1,3-butadiene (C_4H_6-1,3) during the ignition of 2-hexene at a normalized time of $t/\tau_{ign} = 0.90$. Simulations were calculated with the Mehl et al. mechanism at average compositions and conditions of the experiments. Boxes indicate stable compounds in the reaction pathways.

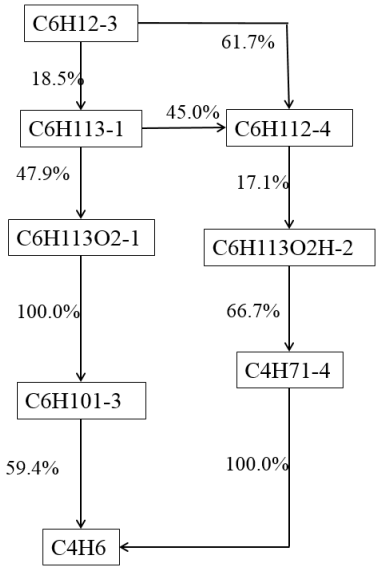

Figure S20. Reaction pathways based on the rate of production analysis for 1,3-butadiene (C_4H_6-1,3) during the ignition of 3-hexene at a normalized time of $t/\tau_{ign} = 0.90$. Simulations were calculated with the Mehl et al. mechanism at average compositions and conditions of the experiments. Boxes indicate stable compounds in the reaction pathways.